**ASME International Mechanical Engineering Congress and Exposition**
**November 5-10, 2006 Chicago, Illinois**

# IMECE2006-14396

# INPUT SHAPING FOR NONLINEAR DRIVE SYSTEMS

**Thomas H. Bradley, Terry Hall, Qiulin Xie, William Singhose, Jason Lawrence**
Georgia Institute of Technology
Woodruff School of Mechanical Engineering
801 Ferst Drive, Atlanta, Georgia 30332-0405

## ABSTRACT

Input shaping is effective at eliminating vibration in many types of flexible systems. This paper discusses how input shaping is affected by actuators with unequal acceleration and deceleration dynamics. It is shown that traditional Unity Magnitude Zero Vibration (UMZV) shapers have degraded performance when used with such actuators. A new type of UMZV shaped input command is developed to compensate for the nonlinearity. Experiments on a portable bridge crane demonstrate the effectiveness of the proposed approach.

## INTRODUCTION

Real world systems always contain non-linear actuator dynamics. These nonlinearities can often be ignored because their effects are small. However, under certain circumstances, the nonlinearities can influence the effectiveness of the control system. For example, input shaping is very effective at reducing vibration in flexible systems, but, if the calculated input cannot be accurately reproduced by the actuator, then some residual vibration will occur [1,2,3,4]. This paper presents methods for modifying input shaping to work on systems with a certain type of non-linear actuator. The non-linear actuator dynamics studied in this paper are unequal acceleration, $\tau_a$, and deceleration, $\tau_d$, time constants.

Input shaping works by convolving a sequence of impulses with the reference command. These impulses, called the input shaper, filter out problematic frequencies from the input command. One type of input shaper contains impulses whose magnitudes are {+1, -1, +1} [5]. If this Unity Magnitude, Zero Vibration (UMZV) shaper is convolved with a pulse input, of width $t_p$, then the shaped command is as shown in Figure 1.

Figure 1 also shows the effect of non-linear actuator dynamics on the UMZV command. Several problems exist with the use of conventional input shaping on this non-linear system. When the acceleration time constant is large, the full signal amplitude may not be reached between changes in the command. When the acceleration and deceleration time constants differ, the vibration caused by the positive accelerations will not cancel the vibration caused by the negative accelerations. The gain and phase of the resulting vibration will be modified by the actuator time constants.

In order to address these shortcomings of UMZV input shapers, Lawrence et al., analytically derived a unity magnitude, input shaped command that partially compensates for the non-linearity in question [6]. This compensated Unity Magnitude Zero Vibration ($UMZV_C$) command effectively reduces the residual vibration associated with this non-linearity over a limited range of pulse widths, natural frequencies and time constants.

To improve the applicability and effectiveness of unity magnitude commands for this non-linearity, this paper presents and evaluates a numerically derived optimal unity magnitude input shaped command ($UMZV_O$). First, we present the experimental setup used to evaluate the effectiveness of the shaped commands. The numerical simulation used to derive and simulate the response of a system to input shaped commands is then described. We present the characteristics of the UMZV and $UMZV_C$ input shapers and the derivation of the $UMZV_O$ shaped commands. The response of the UMZV, $UMZV_C$ and $UMZV_O$ shaped commands are then compared in simulation. Two methods for applying the $UMZV_O$ input shaped command to real systems are described and evaluated. Simulation validation and experimental comparison of the $UMZV_O$ and other input shapers are then presented.

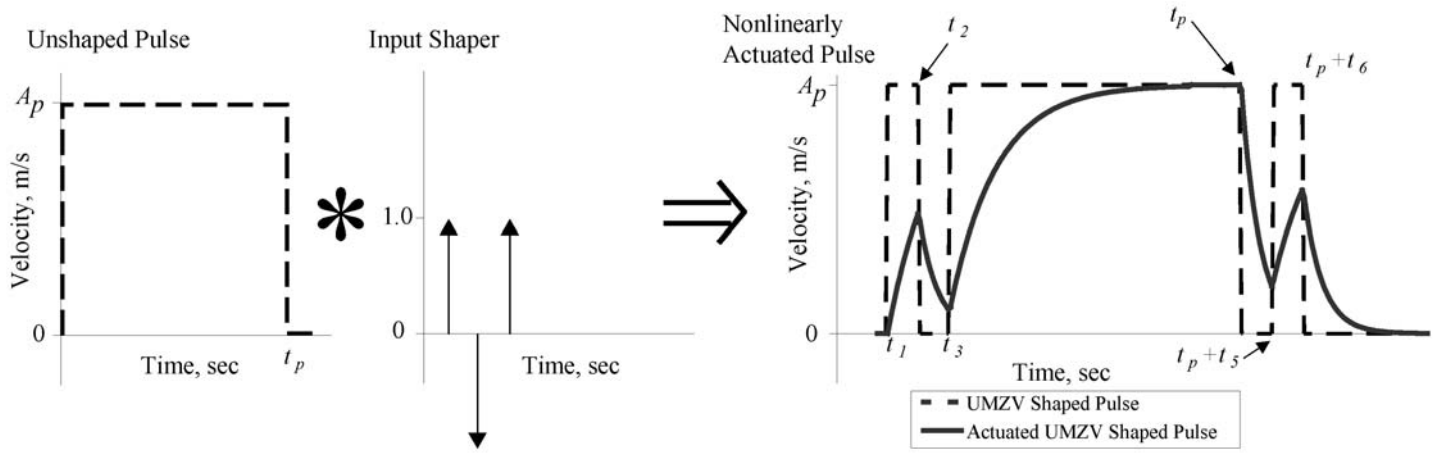


**Figure 1. Commanded and actual output from the non-linear actuator system**

## EXPERIMENTAL SETUP

A portable bridge crane is used in this study for experimental investigation of the effect of a drive system nonlinearity. The portable bridge crane, shown in Figure 2, is a 1m x 1m x 1m miniature bridge crane that is actuated by Siemens motors, drives, and programmable logic controller (PLC). A vision system measures the displacement of the bridge crane payload relative to the bridge trolley [7]. The controller for the portable bridge crane provides commands to the bridge trolley actuator at a frequency of 50Hz.

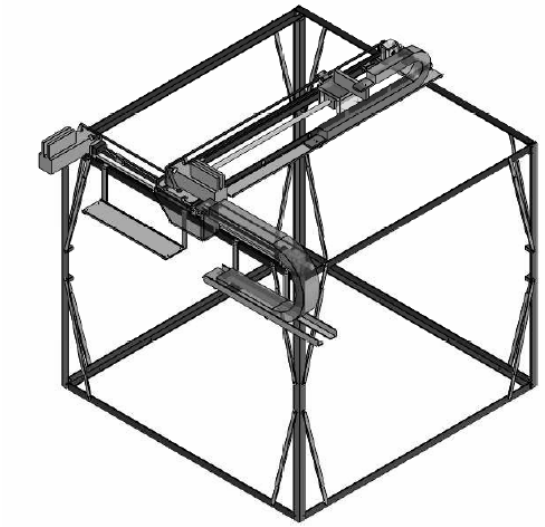

**Figure 2. Portable bridge crane experimental setup**

Figure 3 shows a block diagram of the experimental system. The system is composed of three main physical components: the PLC, the gantry trolley, and the payload. The PLC receives a velocity command, $v_{ref}$, and convolves that command with a UMZV input shaper. The shaped velocity command is an input to the trolley actuator which drives the trolley to produce the trolley velocity, $v_{actual}$. The trolley velocity excites motion of the payload. The position of the payload relative to the position of the trolley, *y,* is the measured output of the system.

As constructed, the portable bridge crane does not exhibit the non-linearity that is investigated in this study, to a significant degree. In order to replicate the actuator nonlinearities on the portable crane, appropriately shaped trolley velocity profiles must be uploaded to the crane's PLC. In this way the time constants of the system can be varied without physical modification of the portable bridge crane.

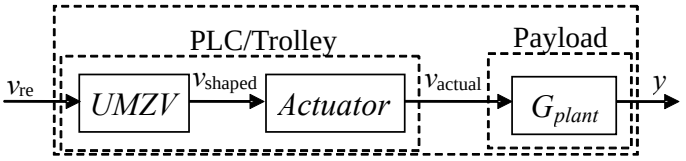


**Figure 3. Physical and functional (italics) block diagram of the portable bridge crane system**

## NUMERICAL SIMULATION

In order to develop and evaluate control algorithms for the portable bridge crane, a numerical simulation of the portable bridge crane system was constructed in the *MATLAB*™/*Simulink*™ environment. Initialization files provide the input shaper impulse times, actuator time constants, and system natural frequency to a *Simulink*™ simulation. The model consists of two serially connected mathematical models that correspond to the physical components of the system shown in Figure 3. The PLC/Trolley model uses the times calculated in the preprocessing routine to coordinate the timing of a series of velocity steps. The velocity steps are filtered through a non-linear first-order system to produce the velocity output of the actuator. The payload model uses the velocity output of the PLC/Trolley model as input and produces the simulated response. The vibration of the payload, as measured from the trolley of the bridge crane, is modeled using the transfer function:

$$G_{plant}(s) = \frac{s}{s^2 + \omega_n^2}, \quad (1)$$

where $\omega_n$ is the natural frequency of the payload oscillation.

The simulation of the input shapers and system is performed as a continuous time simulation. No time discretization of the control system is performed.

## UMZV AND UMZV$_C$ INPUT SHAPERS

Figure 1 showed the fundamental process of shaping a pulse command using a UMZV-type input shaper. The resulting command has six switch times. Given a desired velocity pulse width, $t_p$, the switch time sequence for all of the UMZV-type shaped commands considered in this study is:

$$\begin{bmatrix} A_i \\ t_i \end{bmatrix} = \begin{bmatrix} 1 & -1 & 1 & -1 & 1 & -1 \\ 0 & t_2 & t_3 & t_p & t_p + t_5 & t_p + t_6 \end{bmatrix}, \quad (2)$$

where $t_p$ is the unshaped command pulse duration, $A_i$ is the amplitude of the change of the input and $t_i$ is the corresponding time of the change. The unshaped pulse duration, $t_p$, is sets the move distance and is assumed to be determined by the requirements of the crane operator. Therefore, the four variables that must be defined for each shaped command are $t_2$, $t_3$, $t_5$, and $t_6$.

For the UMZV shaper the switch times are: [5]

$$t_2 = t_5 = \frac{1}{6} \cdot \frac{2\pi}{\omega_n} = \frac{T}{6}, \quad (3)$$

$$t_3 = t_6 = \frac{1}{3} \cdot \frac{2\pi}{\omega_n} = \frac{T}{3}, \quad (4)$$

where $T$ is the oscillation period of the system. For the standard linear UMZV input shaper, the acceleration and deceleration dynamics are assumed to be equal, so $t_2$=$t_5$, and $t_3$=$t_6$.

For the UMVZ$_C$ input shaper of Lawrence et al., the times $t_2$ through $t_6$ are given by: [6]

$$t_2 = \frac{1}{\omega_n}\cos^{-1}\left(\frac{\tau_a\sqrt{\omega_n^2 + \frac{1}{\tau_a^2}}}{2\tau_d\sqrt{\omega_n^2 + \frac{1}{\tau_d^2}}}\right) - \tan^{-1}(\tau_d\omega_n) + \tan^{-1}(\tau_a\omega_n), \quad (5)$$

$$t_3 = \frac{2}{\omega_n}\cos^{-1}\left(\frac{\tau_a\sqrt{\omega_n^2 + \frac{1}{\tau_a^2}}}{2\tau_d\sqrt{\omega_n^2 + \frac{1}{\tau_d^2}}}\right), \quad (6)$$

$$t_5 = \frac{1}{\omega_n}\cos^{-1}\left(\frac{\tau_d\sqrt{\omega_n^2 + \frac{1}{\tau_d^2}}}{2\tau_a\sqrt{\omega_n^2 + \frac{1}{\tau_a^2}}}\right) - \tan^{-1}(\tau_a\omega_n) + \tan^{-1}(\tau_a\omega_n), \quad (7)$$

$$t_6 = \frac{2}{\omega_n}\cos^{-1}\left(\frac{\tau_d\sqrt{\omega_n^2 + \frac{1}{\tau_d^2}}}{2\tau_a\sqrt{\omega_n^2 + \frac{1}{\tau_a^2}}}\right). \quad (8)$$

Equations 5-8 are undefined, and the UMZV$_C$ shaper is not usable for the following parameter ranges: [6]

$$\omega_n\tau_d < 0.5\sqrt{(\omega_n\tau_a)^2 - 3} \quad (9)$$

or ,

$$\omega_n\tau_a < 0.5\sqrt{(\omega_n\tau_d)^2 - 3}. \quad (10)$$

## DERIVATION OF UMZV$_O$ INPUT SHAPED COMMANDS

For the non-linearity considered in this study, the shape of the nonlinear actuator output ($v_{actual}$) that is the input to the payload system is uniquely defined by five variables: { $\tau_a$, $\tau_d$, $t_p$, $T$, $A_p$}. The amplitude of vibration of the linear payload system scales linearly with the amplitude of the unshaped pulse ($A_p$). Because the input-shaped system is linear with respect to amplitude of the unshaped pulse, the residual vibration of any undamped, 2nd-order, linear system to a non-linearly actuated UMZV input shaped command can be uniquely defined as a function of the non-dimensional quantities: { $\frac{\tau_a}{T}$, $\frac{\tau_d}{T}$, $\frac{t_p}{T}$ }.

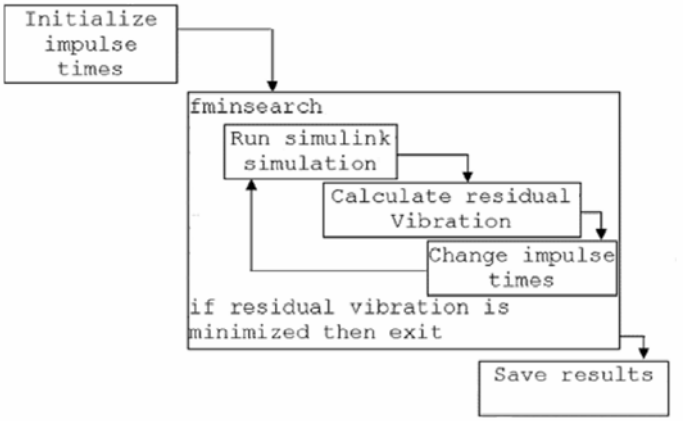


**Figure 4. Flowchart for UMZV$_O$ derivation routine**

Given the limitations of the UMZV and UMZV$_C$ input shapers a new type of UMZV shaped command was designed. Unlike the UMZV$_C$ shaper, for which a formula exists in closed form, this new shaped command (UMZV$_O$) is calculated using numerical optimization. The UMZV$_O$ command was calculated at 1000 evenly spaced points within the 3-dimensional design space:

$$\left\{0.028 \le \frac{\tau_a}{T} \le 0.45\right\} \cap \left\{0.028 \le \frac{\tau_d}{T} \le 0.45\right\} \cap \left\{0.1 \le \frac{t_p}{T} \le 3.0\right\}. \quad (11)$$

At each point within this design space a shaped command optimization routine was run to define optimal values for the four variables {$t_2$, $t_3$, $t_5$, $t_6$} that define a UMZV-type velocity profile. A flowchart of the impulse shaper optimization routine is shown in Figure 4. The impulse times for the conventional

UMZV shaper are used to initialize the optimization routine. The internal *MATLAB*™ program `fminsearch.m` was called to carry out the nonlinear gradient-based optimization routine. The *Simulink*™ simulation was called at each iteration. The optimization cost function that is to be minimized is the residual vibration present in the payload after the trajectory is completed. When the simulated maximum residual vibration reaches a value below 0.1mm, the optimization was stopped, and the values of $\{t_2, t_3, t_5, t_6\}$ were saved to define the $UMZV_O$ command. The derivation of the $UMZV_O$ command was then restarted for the next values of $\frac{\tau_a}{T}$, $\frac{\tau_d}{T}$ and $\frac{t_p}{T}$ within the design space.

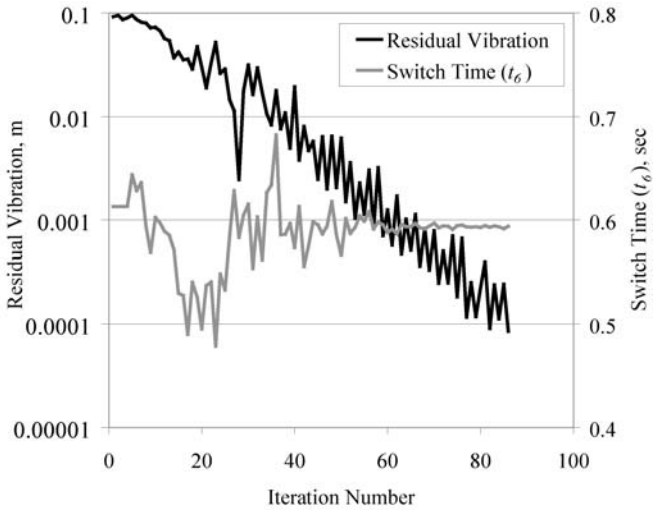


**Figure 5. Convergence and performance sensitivity results for $UMZV_O$ derivation routine**

Figure 5 shows the convergence results of the $UMZV_O$ derivation routine for the sample point $\{\frac{\tau_a}{T}, \frac{\tau_d}{T}, \frac{t_p}{T}\}$ = {0.028, 0.20, 3.0}. The $UMZV_O$ derivation routine requires 86 iterations to reach a convergent solution with residual vibration of less than 0.1mm. As the algorithm executes, the residual vibration of the system is reduced and the average change in the value of the variables $t_2$, $t_3$, $t_5$, and $t_6$ is reduced.

Figure 6 shows the results of the $UMZV_O$ derivation routine after 1 iteration and Figure 7 shows the results of the $UMZV_O$ derivation routine upon completion. As is shown in Figure 5, the residual vibration at iteration 1 is 0.09m, peak to trough. After iteration 86, the residual vibration is less than 0.0001m. Figure 7 shows that the $UMZV_O$ algorithm does not attempt to minimize vibration of the payload during transit, and that even for trajectories where the residual vibration is nearly zero, in-transit deflection can exist.

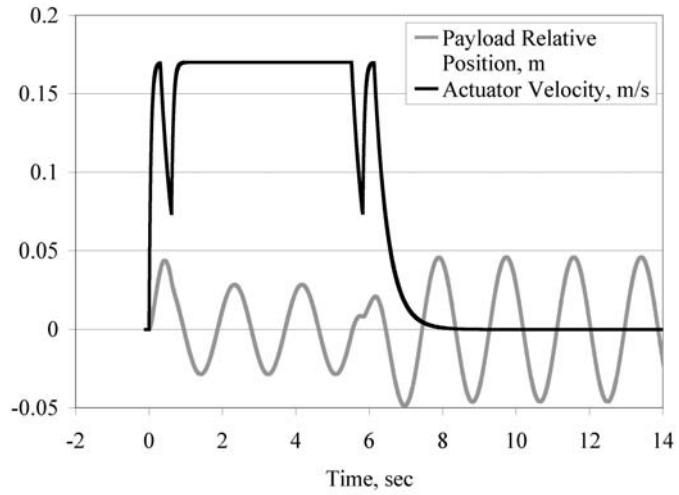


**Figure 6. Simulation results for $UMZV_O$ at iteration 1**

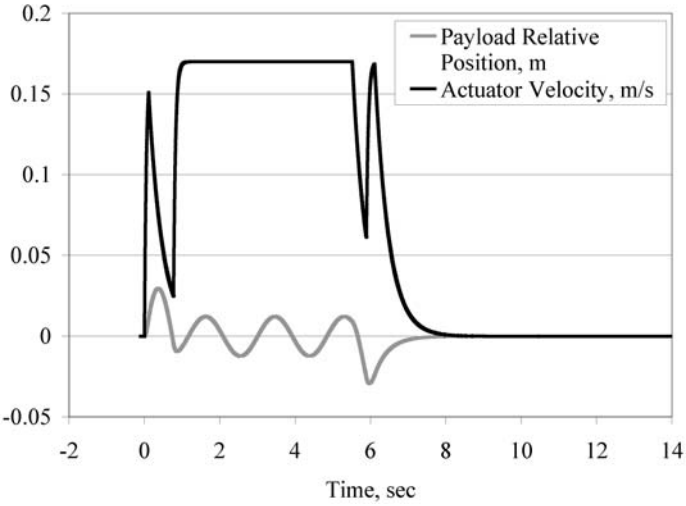


**Figure 7. Simulation results for $UMZV_O$ at iteration 86**

## COMPARISON OF UMZV, $UMZV_C$ AND $UMZV_O$ INPUT SHAPED COMMANDS

To compare the performance of the UMZV, $UMZV_C$ and $UMZV_O$ input shaped commands, the numerical simulation was performed at evenly spaced points within the range of $\frac{\tau_a}{T}$, $\frac{\tau_d}{T}$, $\frac{t_p}{T}$ defined by (11). As stated above, the $UMVZ_C$ input shaper is not defined for values of $\frac{\tau_a}{T}$, $\frac{\tau_d}{T}$, and $\frac{t_p}{T}$ that satisfy (9) and (10). Therefore the response of the $UMZV_C$ shaped system is not evaluated where the shaper is not defined.

Figure 8 shows the simulated residual vibration of the payload system in response to UMZV, $UMVZ_C$ and $UMVZ_O$ shaped inputs. Each subplot shows the dependence of the

system residual vibration on $\frac{\tau_a}{T}$ and $\frac{\tau_d}{T}$ for a fixed value of $\frac{t_p}{T}$. Subplots corresponding to $\frac{t_p}{T}$={0.1, 3.0} are shown for each command.

For each command the residual vibration of the system is nearly zero when $\frac{\tau_a}{T}=\frac{\tau_d}{T}$. Under this condition, the actuated system behaves linearly, all of the input shapers are equivalent to the standard UMZV, and the system exhibits no residual vibration.

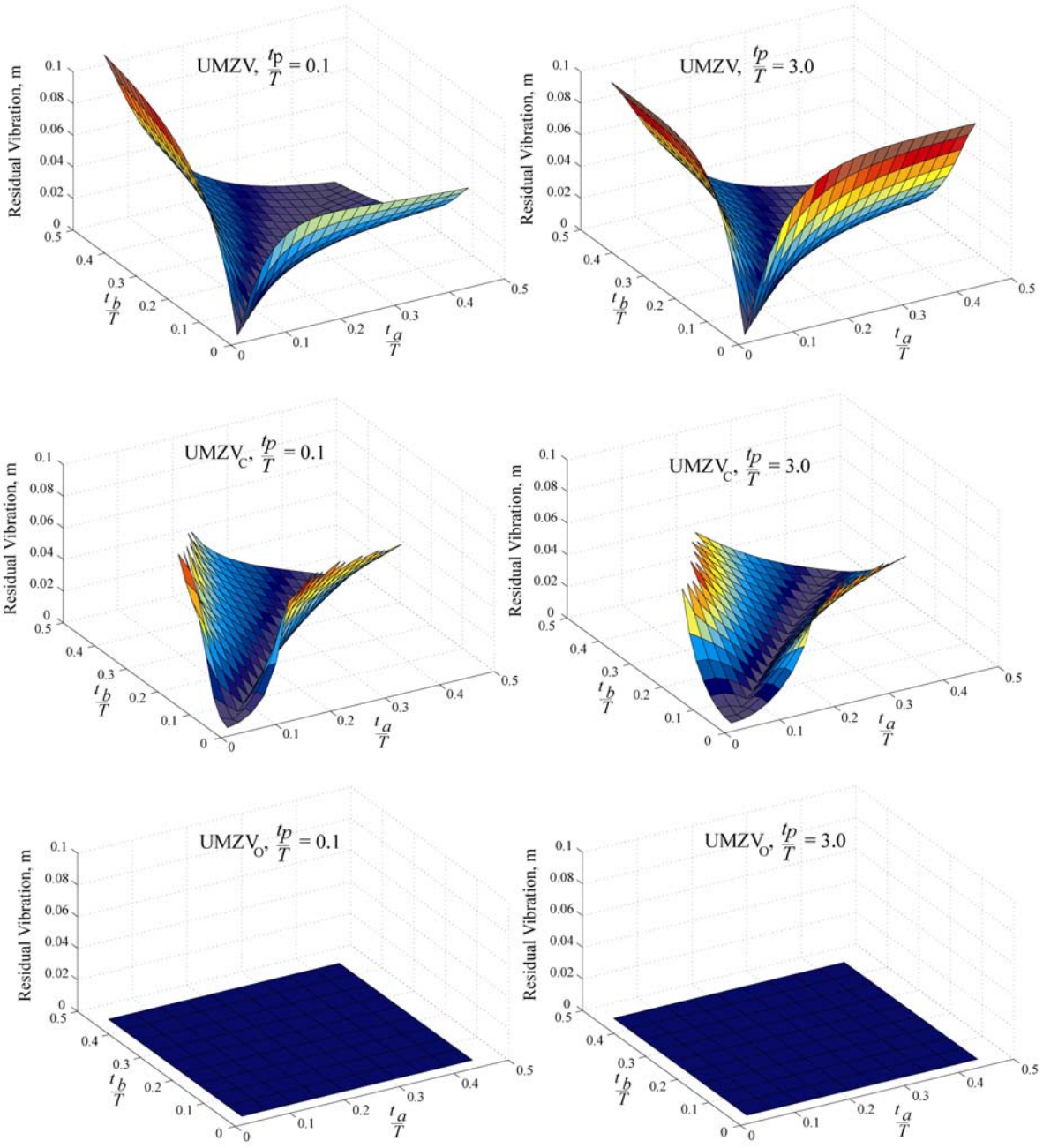


**Figure 8. Numerical comparison of simulated residual vibration for UMZV, UMZV$_C$ and UMZV$_O$ input shaped start-stop trajectories**

Both the UMZV and UMVZ$_C$ show significant residual vibration for other regions of the design space investigated for this study. On the other hand, the residual vibration of the UMVZ$_O$ is approximately 0.1mm for the entire design space.

Comparison of the performance of the UMZV and $UMVZ_C$ input shapers shows that the $UMVZ_C$ is more robust to a wider variety of $\frac{\tau_a}{T}$ and $\frac{\tau_d}{T}$. For regions of the design space where $\{\frac{\tau_a}{T} < 0.22\} \cap \{\frac{\tau_d}{T} < 0.22\}$, the residual vibration associated with the UMZV input shaper increases quickly as one moves away from the line at $\frac{\tau_a}{T} = \frac{\tau_d}{T}$. In these same regions, the residual vibration to the $UMVZ_C$ command is much lower than to the UMZV command. This is especially true for the case where $\frac{t_p}{T}$=3.0. This region where the $UMZV_C$ exhibits significant improvement over the UMZV corresponds to the region where the equations used by Lawrence et al. [3] to derive the $UMZV_C$ shaper are valid, that is where $\frac{t_p}{T} \geq \frac{1}{3} + 3\frac{\min(\tau_a, \tau_d)}{T}$.

## IMPLEMENTATION OF $UMZV_O$ COMMANDS

As shown by the simulation results, when the $UMZV_O$ input shaper is implemented perfectly it is possible to reduce the residual vibration of the non-linearly actuated system to nearly zero. Because derivation of the $UMZV_O$ is computationally costly, it is unlikely that the $UMZV_O$ can be derived and implemented in real time to reduce the vibration of unplanned or operator-controlled motion.

For systems where input shaping can be applied to a preplanned or repetitive motion, where the system can be accurately modeled and where the bandwidth of the control system is high, the $UMZV_O$ derivation routine can be run in advance. The switch times that define the $UMZV_O$ command $\{t_2, t_3, t_5, t_6\}$ can then be stored and used to form the $UMZV_O$ input shaped commands.

For systems that require unplanned, or operator controlled motion, the computational costs of deriving the $UMZV_O$ in real-time is too high. In these cases a method is required for calculating the switch times that define the $UMZV_O$ command from the characteristics of the unplanned movement $\{\frac{\tau_a}{T}, \frac{\tau_d}{T}, \frac{t_p}{T}\}$. Two methods for performing this calculation, linear interpolation and response surface equations, are demonstrated in this section

First, the impulse times that define the $UMZV_O$ for a discretized design space can be stored in the motion controller. In this study, the $UMZV_O$ shaper switch times were derived for 1000 points within a design space that spans most practical applications of a non-linearly actuated bridge crane. For any unplanned motion, the parameters of the motion ($\frac{\tau_a}{T}$, $\frac{\tau_d}{T}$, $\frac{t_p}{T}$) can be calculated, and the switch times of the $UMZV_O$ can be linearly interpolated between the solutions derived for this study. Real-time linear interpolation between the 1000 points of this database is within the capabilities of many motion controllers.

Second, a response surface equation can be fit to the impulse times that define the $UMZV_O$ as a function of the parameters of the motion. The regression coefficients associated with the response surface equations can be stored in the motion controller and approximate values of the $UMZV_O$ impulse times can be calculated in real time. A 2nd-degree response surface equation of the form:

$$Q = b_0 + \sum_{i=1}^{3} b_i x_i + \sum_{i=1}^{3} b_{ii} (x_i)^2 + \sum_{i=1}^{2} \sum_{j=2}^{3} b_{ij} (x_i x_j), \quad (12)$$

was fit to the data for each of the impulse times. The $b_{ij}$ are the regression coefficients, $Q$ is the switch times and $\{x_1, x_2, x_3\} = \{\frac{\tau_a}{T}, \frac{\tau_d}{T}, \frac{t_p}{T}\}$. The $R^2$ values for these fits are no greater than 0.7, indicating a rather poor fit, because of discontinuities in the $\frac{t_p}{T}$ direction.

**Table 1. Time constants and pulse widths used in experimental and numerical comparison**

| Experiment Number | $\frac{\tau_a}{T}$ | $\frac{\tau_d}{T}$ | $\frac{t_p}{T}$ |
|---|---|---|---|
| 1 | 0.187 | 0.123 | 2.03 |
| 2 | 0.150 | 0.135 | 1.55 |
| 3 | 0.113 | 0.147 | 1.06 |
| 4 | 0.077 | 0.158 | 0.583 |
| 5 | 0.040 | 0.170 | 0.100 |

In order to compare the effectiveness of these two methods of implementing the $UMZV_O$ commands, a subset of the tested range of time constants was chosen for further analysis. The position of the subset within the design space is shown in Table 1. These points lie along a line in the three dimensional design space $\{\frac{\tau_a}{T}, \frac{\tau_d}{T}, \frac{t_p}{T}\}$. The shaped response of the system is simulated continuously along the line between experiment 1 and experiment 5. Experiments using the portable bridge crane confirm the performance of the $UMZV_O$ commands at 5 discrete points along that line.

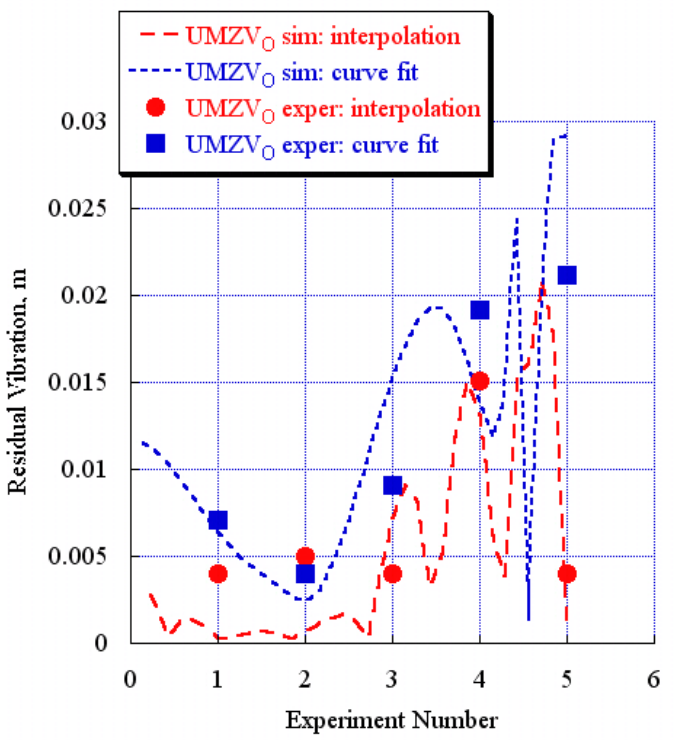


**Figure 9. Simulated and experimental responses of payload**

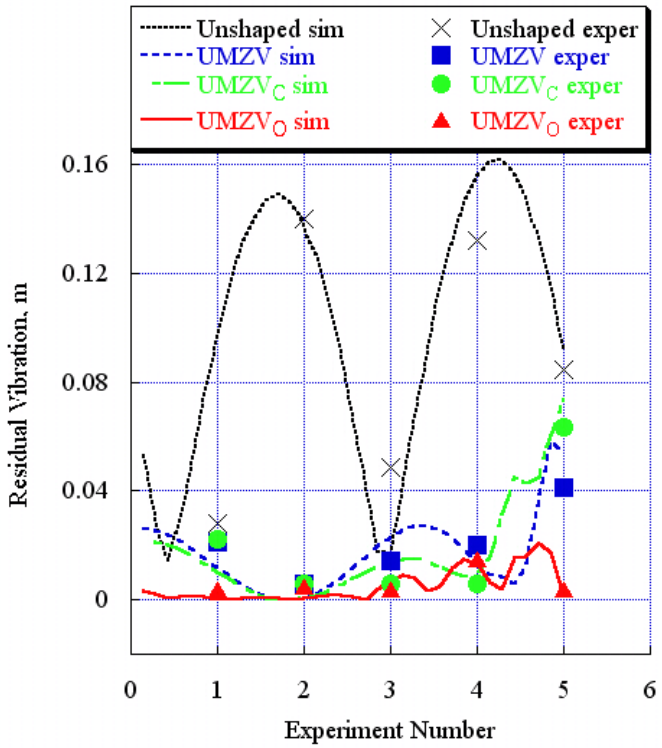


**Fig 10. Simulated and experimental responses of payload**

Figure 9 shows a comparison between the two methods of real-time implementation of the UMZV$_O$ shaped commands. The interpolated UMZV$_O$ commands show lower residual vibration amplitude than does the curve fit UMZV$_O$ commands. In both cases, the experimental data agrees with the simulated response of the systems fairly well. The linear interpolation method is chosen as the most effective method of real-time implementation of the UMZV$_O$ commands and is used exclusively for the following comparisons to the UMZV and UMZV$_C$ input shapers.

## EXPERIMENTAL AND NUMERICAL COMPARISONS

To compare the effectiveness of the UMZV, UMZV$_C$, and UMZV$_O$ shaped commands, the same set of points shown in Table 1 is utilized for further investigation. Again, the response of the shaped response of the system is simulated continuously along the line between experiment 1 and experiment 5. Experiments using the portable bridge crane confirm the performance of the shaped commands at 5 discrete points along that line.

The curves in Figure 10 compare the simulated response and the experimental response for an unshaped command, a UMZV shaped command, a UMZV$_C$ shaped command, and a UMZV$_O$ shaped command. The vertical axis of Figure 10 is a measure of the peak-to-peak vibration of the crane's payload after the trolley has reached the desired location.

The primary result of the experimental comparison of the input shapers is that all of the input-shaped commands show significantly less residual vibration than the unshaped command for this non-linear system. The responses shown in Figure 10 also demonstrate that while the UMZV$_C$ shaper is more robust to changes in the acceleration and deceleration time constants than the UMZV shaper, the UMZV$_O$ shaper outperforms both of them for a majority of the experiments. The results also show fairly good agreement between the experimental and simulated responses for all commands and under all conditions.

## CONCLUSION

The actuator non-linearity caused by unequal acceleration and deceleration time constants has a detrimental effect on the effectiveness of UMZV-type input shapers. A numerically optimized UMZV shaped command (UMZV$_O$) was derived and shown to be effective at reducing residual vibration over a wide range of acceleration time constants, deceleration time constants, frequencies of oscillation and pulse widths. The residual vibration of the numerically optimized UMZV is compared to that of the standard UMZV and a UMZV analytically designed to compensate for this nonlinearity (UMZV$_C$). Methods of implementation of the UMZV$_O$ were considered and compared for effectiveness. The effectiveness of the proposed approach was experimentally validated using a portable bridge crane.

## ACKNOWLEDGMENTS

The authors would like to thank Siemens Energy and Automation for providing the equipment and funding for this research.

## REFERENCES

[1] N. C. Singer and W. P. Seering, “Preshaping command inputs to reduce system vibration,” Journal of Dynamic Systems, Measurement, and Control, vol. 112 , pp. 76-82, 1990.

[2] S. P. Bhat and D. K. Miu, “Precise point-to-point positioning control of flexible structures,” Journal of Dynamic Systems, Measurement, and Control, vol. 112, pp. 667-674, 1990.

[3] B. R. Murphy and I. Watanabe, “Digital shaping filters for reducing machine vibration,” IEEE Transactions on Robotics and Automation, vol. 8, pp. 285-289, 1992.

[4] O. J. M. Smith, “Posicast control of damped oscillatory systems,” Proceedings of the IRE, vol. 45, pp. 1249-1255, 1957.

[5] W. Singhose, N. Singer and W. Seering, “Time-optimal negative input shapers,” J. of Dynamic Systems, Measurement, and Control, vol. 119, pp. 198-205, 1997.

[6] J. Lawrence, J. Danielson and W. Singhose, “Design and analysis of input shapers for systems with a braking nonlinearity,” Submitted to International Symposium on Flexible Automation, Osaka, Japan, 2006.

[7] J. Lawrence and W. Singhose, “Design of a minicrane for education and research,” in 6th International Workshop on Research and Education in Mechatronics, Annecy, France, 2005, pp. 254–259.